Low Contact Resistance Series MEMS Switches

Dimitrios Peroulis, Kamal Sarabandi, and Linda P. B. Katehi
Radiation Laboratory, Electrical Engineering and Computer Science Department,
University of Michigan, 1301 Beal Avenue, Ann Arbor, MI 48109-2122

Abstract— **This paper reports on the design and development of a novel DC-contact MEMS switch for microwave applications. The switching operation utilizes two different forces: electrostatic and stress-induced forces. The former is employed as the actuation force, while the latter is responsible for achieving the actual DC contact. In particular, when no bias voltage is applied, the deformation of a metallic cantilever beam caused by residual gradient stress leads to a metal-to-metal contact. On the other hand, when a DC-voltage is applied between the cantilever beam and an actuation electrode, the cantilever deflects due to electrostatic force and the metallic contact ceases to exist. Contact resistance of less than 1 Ω is demonstrated with this technique in the closed position, which corresponds to an RF insertion loss of 0.1–0.2 dB up to 40 GHz. In this switch the contact force does not depend on the actuation voltage and there is no DC potential across the closed contact, which constitute the main advantages of this design.**

I. Introduction

METAL -to-metal contact MEMS switches and microrelays have received significant attention over the past few years. Several different designs with outstanding RF performance have been developed [1]-[4] that typically rely on electrostatic or thermal actuation mechanisms. Moreover, in all cases the actuation force is also used as the contact force between the two metals of the DC contact. Although it has been demonstrated that low contact resistance can be obtained by this method, a significant over-drive of the switch may be necessary. For instance, whereas a bias voltage of 36 V is enough to activate the switches in [1], it was only when it reached 80 V that a contact resistance of less than 1 Ω was measured. However, such a high voltage severely impacts the switch lifetime by increasing the risk of a mechanical or dielectric failure [5]. Furthermore, metal-to-metal contact switches are typically very sensitive to several fabrication parameters, such as intrinsic stress, because minor inaccuracies during the fabrication process may significantly compromise their achieved performance. Residual gradient stress, for example, may significantly deteriorate the metallic contact and substantially increase the required actuation voltage.

A different approach to designing DC-contact switches that alleviates the aforementioned problems is introduced in this paper. This method relies on 1) de-coupling the actuation and contact forces, and 2) constructively employing gradient stress effects. In particular, electrostatic actuation is still maintained, since it is relatively fast (switching speed in the order of a few μsec) and has very low power requirements. The metal contact, however, is achieved through a stress-originated force. This basic switch idea is presented in Section II, while the fabrication process and the results are presented in Sections III and IV respectively.

II. Switch Design

The basic switch concept is illustrated in Fig. 1. The moving structure is a cantilever beam, which we will refer to as the movable cantilever beam. This beam is fabricated with a high-gradient-stress process that causes a significant upward deflection when the switch is released (Fig. 1a). A second and much stiffer cantilever beam (static beam) is fabricated with a low-stress process above the movable cantilever. Although the two beams are originally separated by a specific distance determined by the fabrication process, the two cantilevers come into direct contact immediately after the structure is released, because of the movable cantilever deflection. The movable and static beams are connected to two RF lines as Fig. 1a shows and thus a closed RF contact is achieved. This is the up- or on-state of the switch. An actuation pad covered by a dielectric layer is also fabricated underneath the cantilevers. The down- or off-state of the switch is realized when a DC potential is applied between the movable cantilever and the actuation pad. If this potential is higher than the movable beam's actuation voltage, this beam deflects and the contact points are separated (Fig. 1b). Although the static cantilever is a very stiff beam, as a precaution it is always maintained at the same potential as the actuation pad. Therefore, this beam does not deflect under the influence of the applied DC bias.

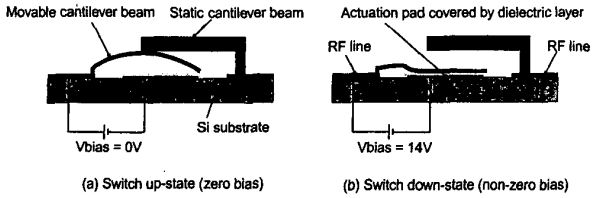

Fig. 1. Basic switch concept and operation. (a) When no bias is applied, the movable cantilever touches the stiff static beam leading to a metal-to-metal contact. (b) If the DC bias is higher than the actuation voltage of the movable beam, this beam deflects downwards leading to an open circuit.

Typically a low on-state insertion loss, high off-state isolation, and low actuation voltage are the desired properties of such a switch. The on-state insertion loss is dominated by the contact resistance, which depends on the movable beam geometry, stiffness, and distance from the static beam. It also depends on the fabrication procedure and especially on the types of metals used and their surface smoothness. On the other hand, the off-state isolation is primarily determined by the distance between the two beams and their overlap area. Finally, because of the mov-

0-7803-7239-5/02/$10.00 © 2002 IEEE

able beam shape and stress, it is difficult to analytically calculate the switch actuation voltage. Nonetheless, a low bound may be obtained assuming that the beam is at a mean distance of D from the actuation pad. Then the following formula [6] for the actuation voltage may be used:

$$V_{min}^{th} = \frac{8}{3}\sqrt{\frac{EID^3}{3\epsilon_0 AL^3}} \quad (1)$$

where E=Young's modulus of the movable beam material, I=same beam moment of inertia, ϵ_0=free space dielectric permittivity, A=effective area between the movable beam and the actuation electrode, and L=movable beam length. Although this formula may be useful for a first hand-calculation, it will only yield a low bound since no stress effects are introduced in it.

III. Fabrication Process

A seven mask process, summarized in Fig. 2, is required for the fabrication of the proposed switch. The process starts with the preparation of a 400 μm silicon substrate with 3000 $\AA$ of SiO_2. A lift-off process is first performed to define the bias lines and the actuation pad. These lines are made of a thin SiCr layer (1200 $\AA$) that is sputtered on top of the negative photoresist [7]. A second lift-off process defines the RF lines, which are made of evaporated Ti and Au layers of 500 and 9000 $\AA$ respectively. Then the actuation pad and bias lines are covered by 4000 $\AA$ of Si_3N_4 deposited by a PECVD process and patterned with a dry RIE etch. A positive photoresist is then spun and patterned to form the first sacrificial layer. For low-actuation voltage switches the thickness of this layer is between 0.8-1.2 μm. The fifth mask is used to define the movable cantilever beam. 2000 $\AA$ of Ti followed by 7000 $\AA$ of Au are evaporated on the whole wafer for this purpose. These layers are subsequently etched except for the locations of the first beam. This is an important step since the induced stress on the beam will determine the deflection magnitude and slope. If the residual gradient stress is not enough, the movable beam will deflect only a few thousand $\AA$, resulting in a poor contact. On the other hand, if excessive stress is introduced, adhesion problems between the movable beam and the sacrificial layer will render the rest of the process impossible.

After this beam is formed, the second sacrificial layer is defined by spinning and soft-baking a 2–2.5 μm layer of polyimide DuPont PI2545. The anchor points for the second beam are then defined similarly to the process reported in [8]. The seed layer (2000 $\AA$ of Au followed by 500 $\AA$ of Ti) necessary for electroplating the second beam is sputter deposited and patterned. It was experimentally found that there is no need for any adhesion layer between Au and polyimide, especially since this layer is only used as a seed layer. Furthermore, an adhesion layer of Ti or Cr underneath the Au layer would deteriorate the desired metal-to-metal contact. The seed layer is then patterned and electroplated to about 6 μm to form a stiff gold beam (static beam). Finally, the two sacrificial layers are etched

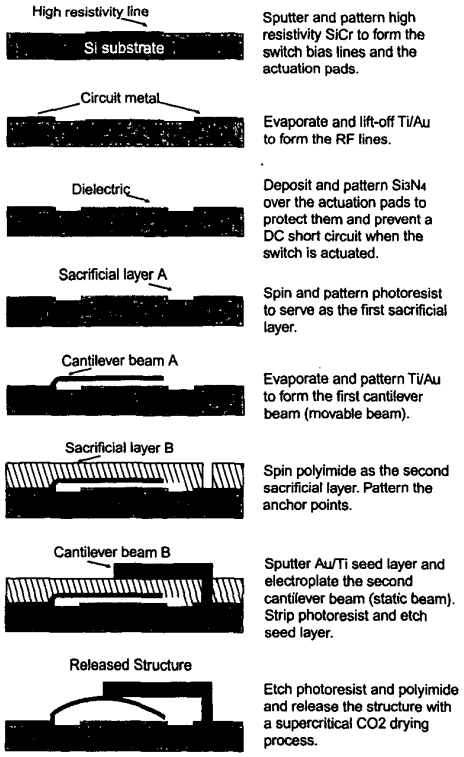

Fig. 2. Process flow for the fabrication of a MEMS switch.

and the structure is dried and released with a standard supercritical CO_2 process.

SEM pictures of three series coplanar waveguide (cpw) switches fabricated with this process can be seen in Fig. 3. The first structure (Fig. 3a) presents a switch with no static beam fabricated. This picture clearly shows the shape of the movable beam after the switch is released. The fabrication process of this beam induces such a stress that its center contacts the static cantilever with a zero slope. This ensures a good and reliable contact. A completed switch with the static beam included is shown in Fig. 3b. The static beam is a low-stress and thick cantilever connected to the left part of the cpw center conductor. A large rectangular hole has been also introduced in this beam in order to minimize the overlap area of the two beams and thus increase the off-state isolation. The movable cantilever is connected to the right part of the center conductor in both structures. Therefore, the two beams become part of the RF circuit in both the up and down states. Finally, the third structure (Fig. 3c) is similar to the second one, except for the movable beam geometry. This beam splits into two parts (secondary movable beams) after the contact point with the static beam. This geometry has the advantage of having a short and thus stiffer static beam. Furthermore, the distance that the RF signal is traveling out of the cpw line is now half of that for the structure of Fig. 3b, which results in less mismatch loss.

Some of the bias details are also visible in these pictures,

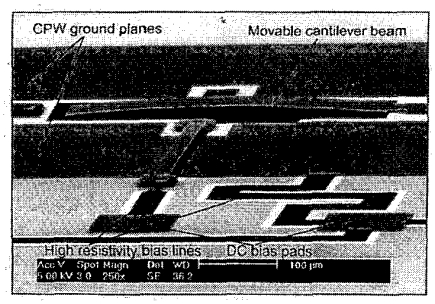

(a) Switch with 500 μm movable beam and no static beam. The maximum beam deflection is approximately 10 μm and occurs at the center of the beam. The switch is fabricated such that the suitable stress is induced on the movable beam, which deflects with the appropriate slope at its center leading to a successful metallic contact.

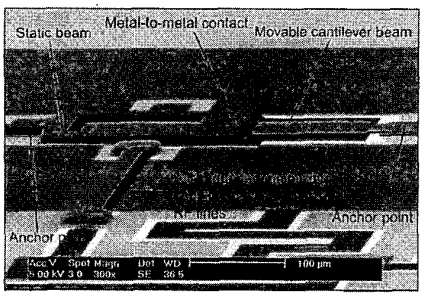

(b) Switch with 300 μm movable beam and 160 μm static beam. A rectangular hole has been introduced in the static beam to minimize the down-state capacitance and increase the isolation.

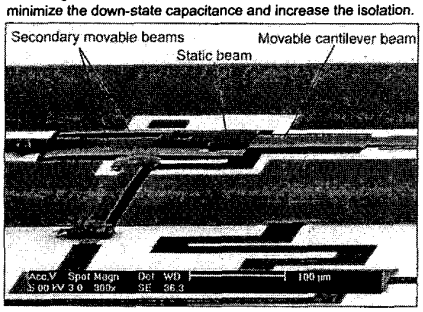

(c) Switch with 300 μm movable beam and 50 μm static beam. The movable beam splits into two parts after the contact with the static beam is made. This results in a short, stiff static beam and shortens the path that the RF signal has to travel out of the cpw.

Fig. 3. SEM pictures of fabricated switches.

which also illustrate the need for high resistance bias lines. In other words, since the bias circuitry comes into direct contact with the RF lines, a strong coupling between the RF and DC signals will occur unless these high resistance lines are introduced.

IV. Results and Discussion

The RF performance of these switches was measured by a 8510C Vector Network Analyzer with the help of an Alessi Probe Station and GGB Picoprobe 150 μm pitch coplanar probes. The effects of the probes and their RF lines to the network analyzer are de-embedded by a standard wideband TRL calibration. Both geometries of Fig. 3b and Fig. 3c gave similar results, but the last one gave a better on-state performance. Fig. 4 presents the measured and simulated

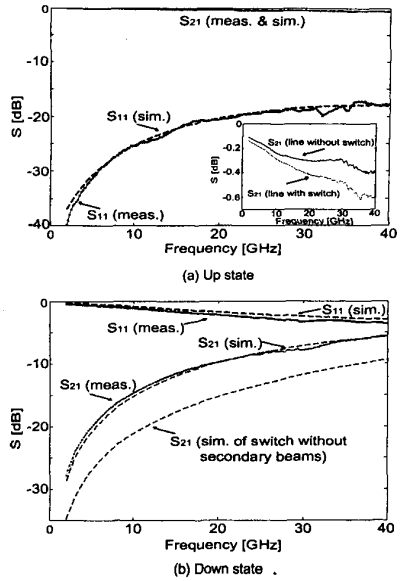

Fig. 4. Measured and Simulated results of the switch shown in Fig. 3c for the (a) up and (b) down state.

RF performance of this geometry.

Fig. 4a shows that the switch presents an up-state insertion loss of 0.14 and 0.38 dB at 2 and 20 GHz respectively. Comparing the low-frequency loss values with a cpw line of the same total length (500 μm) and metallization (0.9 μm of Au), a contact resistance of 0.7 Ω is extracted. Moreover, the measured return loss of the switch is less than -18 dB from 2 to 40 GHz. This slight mismatch is due to the fact that the switch is not at the same level as the cpw line. In other words, although the movable beam is only 3 μm away from the Si substrate at the contact area, it still has a parabolic shape with a mean distance of about $6-7$ μm from the substrate. This is the distance that was used in the full wave simulation [9].

Although outstanding up-state results were presented, the down-state measurements reveal an inferior performance. The measured switch isolation is -28 dB at 2 GHz and remains below -10 dB up to about 20 GHz. This corresponds to a down-state capacitance of approximately 30 fF. However, the photoresist and polyimide thicknesses were 0.8 and 2 μm respectively and, as a result, the theoretical down-state distance between the movable and the static beams is about $d_{th} = 2.8$ μm. Considering that the overlap area between the two beams is 70×30=2100 μm^2, a down-state capacitance of 6.6 fF is calculated using the well-known quasi-static formula. Even if fringing field capacitance is considered, the down-state switch capacitance is still three times smaller than 30 fF. On the other hand, the simulated results agree very well with the experimental values (Fig. 4b) and reveal that the dominant coupling mechanism is not the down-state capacitance, but rather the two secondary beams (Fig. 3c). The simulation was repeated for a hypothetical switch without these two

beams and the results show a 7 dB improvement in the low-frequency switch isolation (Fig. 4b). However, such a switch would only be possible by altering the stress distribution on the movable beam, thus ensuring that this beam would deflect the same way without the secondary beams.

Albeit such a design is possible, the two secondary beams can actually be used to improve the down-state isolation. A brief schematic of this improved switch design is illustrated in Fig. 5a. For clarity purposes, the dielectric and sacrificial layers, as well as part of the biasing details have been omitted from this layout. The extension beams have

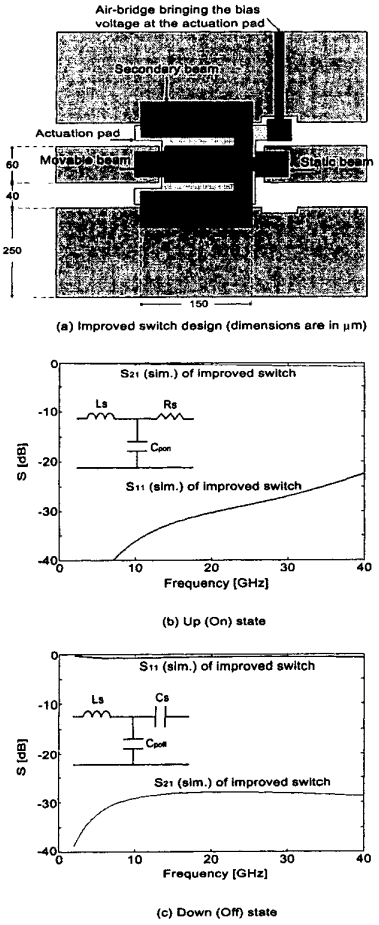

Fig. 5. (a) Simplified layout of improved DC-contact switch design and simulated results for the (b) up- and (c) down-state performance

been 180° rotated in this design resulting in a much reduced coupling with the output (right) port. Moreover, part of these beams are over two sections of the cpw ground planes covered by a thin dielectric layer (3000 $\AA$ of Si_3N_4), not shown in the figure. Therefore, the operation of the switch is as follows. When no DC bias is applied, the movable beam is touching the static beam resulting in a DC-contact (R_s). Due to the residual stress, the secondary beams are far away from the ground plane (estimated mean distance of 5−6 μm according to Fig. 3c) and as a result, a small parasitic shunt capacitance is introduced (C_{pon}). On the other hand, the movable beam, as well as the secondary beams, deflect when a DC bias is applied. However, not only is a small series capacitance (C_{soff}) introduced this time, but also a large shunt capacitance (C_{poff}). This last capacitance is due to the secondary beams that short-circuit the input signal. This mechanism is very similar to the well-known shunt-series switch configuration, but it is achieved by only one switch in this design. The simulated down-state switch performance (Fig. 5c) is substantially improved compared to the previous switch. The off-state isolation is better than −28 dB from 2 to 40 GHz. In addition, the up-state return loss is better than −20 dB for the same bandwidth. The measured performance of this switch will be presented in the conference.

V. Conclusions

A novel design scheme for metal-to-metal contact RF MEMS switches has been introduced. These switches are electrostatically actuated, but the DC-contact is achieved through a stress-originated force. The contact resistance is not related to the actuation force and thus low-voltage DC-contact switches are feasible. A contact resistance of less than 1 Ω with 14 V actuation voltage has been demonstrated with this technique. Finally, a very wideband series-shunt switch configuration using only one MEMS switch has been proposed.

Acknowledgments

This work has been supported by Lockheed-Martin under the RECAP program.

References

[1] S. Duffy, C. Bozler, S. Rabe, J. Knecht, L. Travis, P. Wyatt, C. Keast, M. Gouker, *MEMS Microswitches for Reconfigurable Microwave Circuitry*, IEEE Microwave and Wireless Components Letters, vol. 11, no. 3, March 2001, pp. 106-8.

[2] R. E. Mihailovich, M. Kim, J. B. Hacker, E. A. Sovero, J. Studer, J. A. Higgins, J. F. DeNatale, *MEM Relay for Reconfigurable RF Circuits*, IEEE Microwave and Wireless Components Letters, vol. 11, no. 2, February 2001, pp. 53-55.

[3] P. M. Zavracky, N. E. McGruer, R. H. Morrison, D. Potter, *Microswitches and Microrelays with a View Toward Microwave Applications*, International Journal of RF and Microwave Computer Aided Engineering, vol. 9, no. 4, July 1999, pp.338-47.

[4] D. Hyman, J. Lam, B. Warneke, A. Schmitz, T. Y. Hsu, J. Brown, J. Schaffner, A. Walston, R. Y. Loo, M. Mehregany, J. Lee, *Surface-Micromachined RF MEMS Switcheson GaAs Substrates*, International Journal of RF and Microwave Computer Aided Engineering, vol. 9, no. 4, July 1999; p.348-61.

[5] C. Goldsmith, J. Ehmke, A. Malczewski, B. Pillans, S. Eshelman, Z. Yao, J. Brank, M. Eberly, *Lifetime Characterization of Capacitive RF MEMS Switches*, IEEE MTT-S International Microwave Symposium Digest, vol. 1, June 2001, pp. 227-30.

[6] Y. Loke, G. H. McKinnon, M. J. Brett, *Fabrication and Characterization of Silicon Micromachined Threshold Accelerometers*, Sensors and Actuators A (Physical), vol. A29, no. 3, Dec. 1991, pp. 235-40.

[7] J. B. Muldavin, G. M. Rebeiz, *All-Metal High-Isolation Series and Series/Shunt MEMS Switches*, IEEE Microwave and Wireless Components Letters, vol. 11, no. 9, Sept. 2001, pp.373-5.

[8] S. Pacheco, L. P. B. Katehi, C. T. Nguyen, *Design of Low Actuation Voltage RF MEMS Switch*, ,IEEE International Microwave Symposium Digest, vol.1, June 2000, pp. 165-168.

[9] Zeland's IE3D, Release 7, 2000.